Preprints of the 21st IFAC World Congress (Virtual)
Berlin, Germany, July 12-17, 2020

Identification of continuous-time systems utilising Kautz basis functions from sampled-data ⋆

María Coronel [*,**] **Rodrigo Carvajal** [*] **Juan C. Agüero** [*]

[*] *Electronics Engineering Department, Universidad Técnica Federico Santa María (USM)*
[**] *Electrical Engineering Department, Universidad de Los Andes, Venezuela*

Abstract: In this paper we address the problem of identifying a continuous-time deterministic system utilising sampled-data with instantaneous sampling. We develop an identification algorithm based on Maximum Likelihood. The exact discrete-time model is obtained for two cases: i) known continuous-time model structure and ii) using Kautz basis functions to approximate the continuous-time transfer function. The contribution of this paper is threefold: i) we show that, in general, the discretisation of continuous-time deterministic systems leads to several local optima in the likelihood function, phenomenon termed as *aliasing*, ii) we discretise Kautz basis functions and obtain a recursive algorithm for constructing their equivalent discrete-time transfer functions, and iii) we show that the utilisation of Kautz basis functions to approximate the true continuous-time deterministic system results in convex log-likelihood functions. We illustrate the benefits of our proposal via numerical examples.

Keywords: System identification, Continuous-time model, Maximum Likelihood, Discrete-time model, Kautz basis functions.

1. INTRODUCTION

Identification of continuous-time (CT) systems has been studied in different areas of research such as System Identification and Control of Linear Systems (Åström et al., 1984; Garnier and Wang, 2008; Yuz et al., 2011; Ljung and Wills, 2010; Goodwin et al., 2013; Chen et al., 2017), Identification of Nonlinear Systems (Laila and Astolfi, 2006), Signal Processing (Kirshner et al., 2011), Vibration Analysis (Prior and de Oliveira, 2014; González et al., 2018) and Time Series Analysis (Simos, 2008), among others.

In some applications model structure (number of poles, and zeros) of CT systems is known (see e.g. Tzeng et al. (2001); Rojas et al. (2014)). However, when the model structure is unknown, Basis Functions (BFs) can be used to obtain accurate models represented by few parameters (Heuberger et al., 2005). This approach has been tailored in control theory and system identification, specifically, using Laguerre and two-parameter Kautz BFs (Kautz, 1954; Wahlberg, 1994; Wahlberg and Mäkilä, 1996).

On the other hand, several methods to identify CT systems have been developed from the corresponding discrete-time (DT) model (Wahlberg, 1988; Ljung and Wills, 2010; Goodwin et al., 2013). This approach is known as *Indirect method*. Since the mapping from CT system parameters to the corresponding sampled-data model is highly complex, approximated DT models are obtained in this approach by using i) fast sampling ($\Delta \to 0$), ii) Euler transformation or iii) Bilinear transformation (see e.g. Åström et al. (1984); Yuz et al. (2011); Heuberger et al. (1995)).

In the Maximum Likelihood (ML) framework to identify CT systems utilising sampled-data, the log-likelihood function presents, in general, several local maxima (Kirshner et al., 2011; Chen et al., 2017; González et al., 2018)). It has been shown that the location and number of local optima changes when the sampling process is modified (e.g. when the sampling period changes or irregular sampling is introduced). This phenomenon was termed as *aliasing* (Kirshner et al., 2011) for stochastic systems. This *aliasing* effect makes it difficult to optimize the log-likelihood function, especially when slow sampling is used (for more details see Kirshner et al. (2011); Chen et al. (2017); González et al. (2018)).

In the recent paper (Coronel et al., 2019) a methodology to identify CT deterministic systems represented by Laguerre BFs from sampled-data was presented. In this approach the exact equivalent DT system was utilised. This approach exhibits good accuracy in the estimation for fast and slow sampling. Nevertheless, the estimation accuracy is limited to approximating CT systems without complex poles.

In this paper, we propose an identification algorithm based on the ML framework for CT deterministic systems with complex poles using exact DT models and finite

⋆ The work of María Coronel was supported by ANID/Doctorado Nacional/2017-21170804 and the PIIC at USM No. 004/2019. The work of Rodrigo Carvajal and Juan C. Agüero was supported by FONDECYT trough grant No 1181158. This work was supported by ANID-Basal Project FB0008.

sample period. We analyse two cases: i) known model structure and ii) Kautz BFs to approximate CT systems. We analyse the log-likelihood function for both cases, extending the concept of *aliasing* in the likelihood function to deterministic systems. In the numerical examples, we observe that only for the case in which known model structure is assumed, the log-likelihood function exhibits several local maxima for slow sampling, whilst by using Kautz BFs the *aliasing* in the log-likelihood function is not present.

The remainder of the paper is as follows: In Section 2 the system of interest is presented. In Section 3 the equivalent DT model is obtained. A numerical example is shown in Section 4. Finally, conclusions are presented in Section 5.

2. SYSTEM OF INTEREST

Consider the following deterministic CT system:

$$y(t) = G(s)u(t), \tag{1}$$

where $y(t)$ denotes the output signal, $u(t)$ is the input signal, s is the time-derivative operator ($s = \frac{d}{dt}$) or the Laplace transform variable, and $G(s)$ is the transfer function (TF).

We utilise a Zero Order Hold (ZOH) and instantaneous sampling with period Δ to obtain the sampled output signal. We assume that the output is given by (Jazwinski, 1970; Ljung and Wills, 2010):

$$\bar{y}(t_k) = G_d(z)u(t_k) + v(t_k), \tag{2}$$

where $\bar{y}(t_k)$ denotes the sampled output signal, $u(t_k)$ is the sampled input signal, z is the forward shift operator or Z-transform variable and $v(t_k)$ is a zero-mean Gaussian white noise sequence with variance σ^2.

It is well known that the log-likelihood function for (2) is given by (Ljung (1999)):

$$\ell(\beta) = -\frac{N}{2}\log\left(2\pi\sigma^2\right) - \frac{1}{2\sigma^2}\sum_{t_k=1}^{N} \varepsilon_{t_k}(\theta)^2, \tag{3}$$

where $\beta = \left[\theta^T \; \sigma^2\right]^T$ is the vector of parameters to be estimated, N is the data length and $\varepsilon_{t_k}(\theta)$ is the prediction error given by

$$\varepsilon(\theta) = \bar{y}(t_k) - G_d(z,\theta)u(t_k). \tag{4}$$

The ML estimator is then given by

$$\hat{\beta}_{\mathrm{ML}} = \arg\max_{\beta} \; \ell(\beta). \tag{5}$$

3. EQUIVALENT DISCRETE-TIME MODEL

3.1 Known second order model structure for the CT system

Consider the following *known model* for the TF in (1):

$$G(s) = \frac{\omega_n^2}{s^2 + 2\zeta\omega_n s + \omega_n^2}, \tag{6}$$

where ω_n is the natural frequency of oscillation and ζ is the damping factor.

From (6), the corresponding sampled-data TF can be obtained as follows (see e.g. Goodwin et al. (2013)):

$$G_d(z) = \left(1 - z^{-1}\right)\mathscr{Z}\left\{\mathscr{L}^{-1}\left[\frac{G(s)}{s}\right]\Bigg|_{t=k\Delta}\right\}, \tag{7}$$

where $\mathscr{L}^{-1}$ is the inverse Laplace transform and $\mathscr{Z}$ is the Z-transform. For completeness of the presentation we present the following result.

Proposition 1. (Åström and Wittenmark, 1984, sec. 2.7) The equivalent discrete-time model of the continuous-time system in (6) is given by:

$$G_d(z) = \frac{\bar{b}_1 z + \bar{b}_2}{z^2 + \bar{a}_1 z + \bar{a}_2}, \tag{8}$$

where

$$\bar{b}_1 = 1 - \alpha\left(B + \zeta\omega_n/\bar{\omega}\right), \; \bar{b}_2 = \alpha^2 + \alpha\left(\zeta\omega_n\gamma/\bar{\omega} - B\right), \tag{9}$$

$$\bar{a}_1 = -2\alpha B, \quad \bar{a}_2 = \alpha^2, \tag{10}$$

with

$$\bar{\omega} = \omega_n\sqrt{1-\zeta^2}, \quad \zeta < 1, \quad \alpha = \exp\left(-\zeta\omega_n\Delta\right), \tag{11}$$

$$B = \cos(\bar{\omega}\Delta), \quad \gamma = \sin(\bar{\omega}\Delta). \tag{12}$$

Remark 2. We note that B and γ depend on the trigonometric functions $\cos(\bar{\omega}\Delta)$, and $\sin(\bar{\omega}\Delta)$ respectively. Thus, an oscillatory behaviour is expected in the log-likelihood function (3), which corresponds to the *aliasing* effect coined in (Kirshner et al., 2011) for stochastic systems.

3.2 Kautz basis functions to approximate the CT system

Kautz BFs have been widely used for systems with complex poles (Wahlberg (1994); Heuberger et al. (1995); Wahlberg and Mäkilä (1996); Baldelli et al. (2001)). They are defined as follows (Wahlberg and Mäkilä, 1996):

$$F_{2i-1}(s) = \frac{\sqrt{2b}s\left(s^2 - bs + c\right)^{i-1}}{\left(s^2 + bs + c\right)^i}, \tag{13}$$

$$F_{2i}(s) = \frac{\sqrt{2bc}\left(s^2 - bs + c\right)^{i-1}}{\left(s^2 + bs + c\right)^i}, \tag{14}$$

where $i = 1, 2, \ldots, n$, $b = 2a$ and $c = a^2 + \omega^2$, a and ω are the real and imaginary part of the complex poles ($a \pm j\omega$), with $a > 0$. Notice that one of the benefits of Kautz BFs are that they can be constructed in a recursive manner.

The TF in (1) can be approximated by using Kautz BFs as follows (Wahlberg and Mäkilä, 1996):

$$\hat{G}(s) = \sum_{i=1}^{n} \hat{w}_{2i-1}F_{2i-1}(s) + \hat{w}_{2i}F_{2i}(s), \tag{15}$$

where n is the number of BFs used, $\hat{w}_{2i-1}$ and $\hat{w}_{2i}$ are the weights associated to the BFs to be estimated and $F_{2i-1}(s)$ and $F_{2i}(s)$ are the Kautz basis TF in (13) and (14). Notice that the terms $\sqrt{2b}$ and $\sqrt{2bc}$ in (13) and (14) respectively, can be included in the weights of Kautz BFs in (15).

The Kautz BFs in (13) and (14) can be expressed in terms of the following recursion:

(1) **for** $i = 1$:

$$F_1 = \frac{s}{s^2 + bs + c}, \quad F_2 = \frac{1}{s^2 + bs + c}. \tag{16}$$

(2) **for** $i \geq 2$:

$$F_{2i-1} = F_{2i-3} + \bar{F}_{2i-1}, \quad F_{2i} = F_{2i-2} + \bar{F}_{2i}, \tag{17}$$

where

$$\bar{F}_{2i-1} = F_{2i-3}\bar{W}, \; \bar{F}_{2i} = F_{2i-2}\bar{W}, \; \bar{W} = \frac{-2bs}{s^2 + bs + c}. \tag{18}$$

Typically the TFs are represented in state-space form for simplicity of the computation and representation. In fact, we base our analysis on the state-space representation of the TF in (18) in order to exploit a particular structure that is obtained. Moreover, this structure allows for defining some terms that yield a recursive structure of the DT versions of Kautz BFs based on (17).

Here we use a general CT state-space representation to obtain the exact DT model:

$$\dot{x}(t) = Ax(t) + Bu(t), \quad y(t) = Cx(t), \tag{19}$$

where the system matrices are constructed with the following recursion corresponding to the space-state matrices of the ith-term in (15) [1]:

(1) **for** $i = 1$:

$$A_1{=}A_2{=}\begin{bmatrix} -b & 1 \\ -c & 0 \end{bmatrix},\ B_1{=}\begin{bmatrix} 1 \\ 0 \end{bmatrix},\ B_2{=}\begin{bmatrix} 0 \\ 1 \end{bmatrix},\ C_1{=}C_2{=}[1\ \ 0]\,. \tag{20}$$

(2) **for** $i \geq 2$: we define the circulant upper triangular (cut) matrix operator :

$$\begin{aligned} \bar{A}_{2i-1} = \bar{A}_{2i} &= \mathrm{cut}(A_{\bar{W}}, B^*, 0_{2\times 2}, \cdots, 0_{2\times 2}), \\ &= \begin{bmatrix} A_{\bar{W}} & B^* & 0_{2\times 2} & \cdots & 0_{2\times 2} \\ 0_{2\times 2} & A_{\bar{W}} & B^* & \cdots & 0_{2\times 2} \\ \vdots & \vdots & \ddots & \ddots & \vdots \\ 0_{2\times 2} & 0_{2\times 2} & \cdots & \ddots & B^* \\ 0_{2\times 2} & 0_{2\times 2} & \cdots & \cdots & A_{\bar{W}} \end{bmatrix}, \end{aligned} \tag{21}$$

$$\bar{B}_{2i-1}{=}[0_{2\times 2}\ 0_{2\times 2} \cdots 1\ \ 0]^T, \bar{B}_{2i}{=}[0_{2\times 2}\ 0_{2\times 2}\ \cdots\ 0\ \ 1]^T, \tag{22}$$

$$\bar{C}_{2i-1} = \bar{C}_{2i} = [1\ \ 0\ \ 0_{2\times 2}\ \cdots\ 0_{2\times 2}]\,, \tag{23}$$

where:

$$A_{\bar{W}} = \begin{bmatrix} -b & 1 \\ -c & 0 \end{bmatrix}, \quad B^* = \begin{bmatrix} -2b & 0 \\ 0 & 0 \end{bmatrix}. \tag{24}$$

Then, the sampled-data model is given by (Bernstein and So, 1993; Goodwin et al., 2013):

$$x(t_{k+1}) = A^d x(t_k) + B^d u(t_k), \quad y(t_k) = Cx(t_k), \tag{25}$$

where $A^d = e^{A\Delta}$ and $B^d = \int_0^\Delta e^{A\eta} B d\eta$.

The exact DT model for Kautz BFs can be obtained using the following result:

Theorem 3. The equivalent discrete-time model of the Kautz Basis Functions are given by:

(1) **for** $i = 1$:

$$F_1^d = \frac{d_2\bar{z} - d_1}{\bar{z}^2 - 2\bar{z}\cos(\omega\Delta) + 1}, \tag{26}$$

$$F_2^d = \frac{e_2 z + e_1}{\bar{z}^2 - 2\bar{z}\cos(\omega\Delta) + 1}, \tag{27}$$

where:

$$\bar{z} = e^{a\Delta} z, \quad d_2 = \sin(\omega\Delta)/\omega, \quad d_1 = e^{a\Delta}\sin(\omega\Delta)/\omega,$$
$$e_2 = (e^{a\Delta}\omega - \omega\cos(\omega\Delta) - a\sin(\omega\Delta))/(\omega(a^2 + \omega^2 1)),$$
$$e_1 = (\omega - \omega e^{a\Delta}\cos(\omega\Delta) + a e^{a\Delta}\sin(\omega\Delta))/(\omega(a^2 + \omega^2 1)).$$

(2) **for** $i \geq 2$:

$$F_{2i-1}^d(z) = F_{2i-3}^d(z) + \bar{F}_{2i-1}^d(z), \tag{28}$$

$$F_{2i}^d(z) = F_{2i-2}^d(z) + \bar{F}_{2i}^d(z), \tag{29}$$

[1] The subscripts refer to the corresponding CT Kautz BFs and $\bar{A}_j$ to the corresponding $\bar{F}_j$ TF of the recursions defined in (17) and (18).

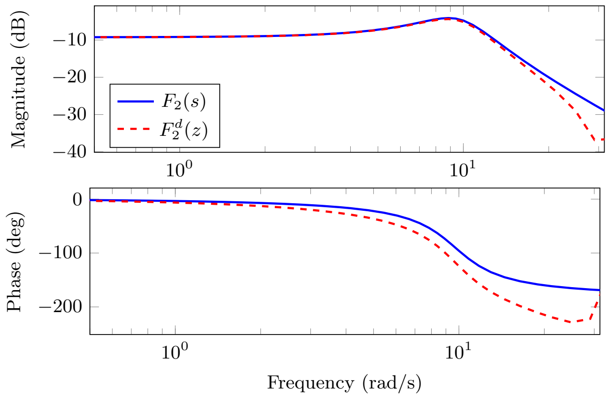

Fig. 1. Frequency Response of CT (F_2) and DT (F_2^d) Kautz BFs for slow sampling.

where:

$$\bar{F}_{2i-1}^d = [1\ \ 0]\left(R^{-1}B_{2i-3}^d + \sum_{k=1}^{2i-3} R^{-1} M_\Delta^k R^{-1} B_{2i-2-k}^d\right), \tag{30}$$

$$\bar{F}_{2i}^d = [1\ \ 0]\left(R^{-1}B_{2i-2}^d + \sum_{k=1}^{2i-2} R^{-1} M_\Delta^k R^{-1} B_{2i-k-1}^d\right), \tag{31}$$

with $R = z - e^{A_{\bar{W}}\Delta}$, $B_{2i-3}^d = \int_0^\Delta e^{\bar{A}_{2i-3}\eta}\bar{B}_{2i-3} d\eta$ and $B_{2i-2}^d = \int_0^\Delta e^{\bar{A}_{2i-2}\eta}\bar{B}_{2i-2} d\eta$. The matrices $A_{\bar{W}}$, $\bar{A}_j$ and $\bar{B}_j$ are given by (24), (21) and (22) respectively.

Proof. See Appendix B. □

From Theorem 3, the DT model of the CT system in (1) is obtained as follows:

$$\hat{G}^d(z) = \sum_{i=1}^n \hat{w}_{2i-1} F_{2i-1}^d(z) + \hat{w}_{2i} F_{2i}^d(z), \tag{32}$$

It can be shown that the discretisation of the CT Kautz BFs results in a concave log-likelihood function, which is simple to optimise. In addition, the recursive nature of the result in Theorem 3 (see (28) and (29)) is useful to reduce the computational complexity, especially when one uses a large number of basis functions.

4. NUMERICAL EXAMPLE

In this section we present a numerical example to illustrate the benefits of our proposal for CT system identification using sampled-data. First, we will compare the frequency response of the CT Kautz BF (F_2) and DT Kautz BF (F_2^d) for slow sampling. Then, we analyse the log-likelihood function given in (3) for two cases, when the model structure is known and when the Kautz BFs are used for approximating the CT system. Finally, for both cases we analyse our approach in an estimation problem using ML. We consider the CT system in (1), in which the TF $G(s)$ is given by (6) with $\omega_n = 10\ rad/s$ and $\zeta = 0.3$, the input signal is zero mean Gaussian distributed with variance $\sigma_u^2 = 10$ and the variance of the DT zero mean Gaussian noise in (2) is $\sigma^2 = 1$. In addition, we consider fast sampling $\Delta = 10$ ms, slow sampling $\Delta = 100$ ms, and data length of $N = 10000$. For the estimation problem we consider 100 Monte Carlo (MC) simulations.

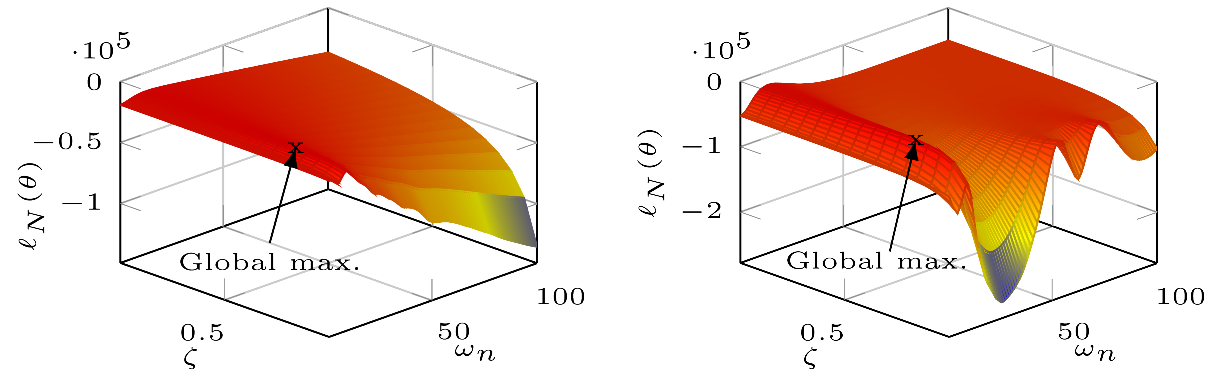

(a) Fast sampling (b) Slow sampling

Fig. 2. Log-likelihood function for case known model structure. For (a) fast sampling and (b) slow sampling.

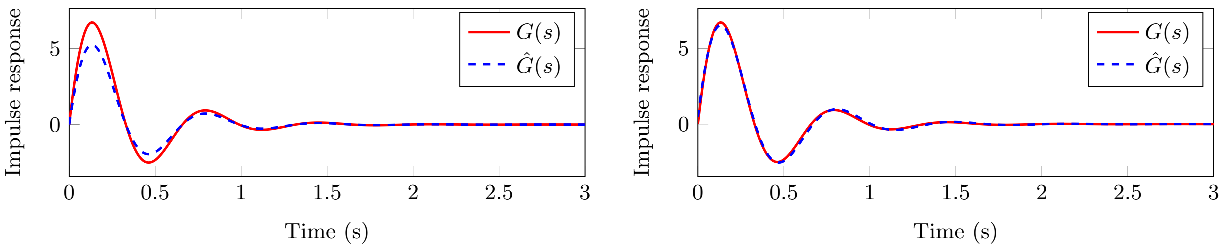

(a) Known model structure (b) Kautz BFs

Fig. 3. Impulse response of the *true* system and mean of the estimated using ML with (a) known model structure and (b) Kautz BFs. For 100 MC simulations and slow sampling.

4.1 Frequency-domain analysis

Fig. 1 shows the magnitude and phase of the frequency response of CT (F_2) and equivalent DT (F_2^d) Kautz BF for slow sampling. It is clear that the behaviour at low frequencies is similar and for higher frequencies we observe a small difference between the CT Kautz BF and its DT version.

4.2 Likelihood function analysis

Fig. 2 shows the log-likelihood function corresponding to fast sampling and slow sampling when the model structure is known. We observe that for slow sampling the log-likelihood function exhibits several local maxima. This effect of *aliasing* in the log-likelihood function hinders the attainment of the global maximum. In this sense, a global optimisation algorithm should be utilised, resulting in a large computational load. In contrast, when the Kautz BFs are used to approximate the CT system, the likelihood function is concave in the region of interest for both slow and fast sampling.

4.3 Maximum likelihood identification

When the model structure is known, we estimate the CT parameters (ζ and ω_n) utilising a global optimisation algorithm to solve the estimation problem. In particular, we use the Generalised Pattern Search (GPS) algorithm of Matlab® based on the mesh adaptive search (MADS) algorithm (Audet and Dennis (2003)). For illustration purposes, we choose a complex pole similar to the true value for the Kautz BFs [2]. In this example we use $a = 2.8$ and $\omega_n = 9.3$ and two Kautz BFs ($n = 2$). We estimate the weights of the basis in (15) utilising a closed form solution.

Fig. 3 shows the impulse response of the *true* system and the mean of the estimations for all MC simulations when the model structure is known and when Kautz BFs are used to approximate the CT system, utilising slow sampling. We observe a good accuracy in the estimation for both cases. Notice that when the model structure is known, the estimation accuracy is affected by the initialisation of the global optimisation algorithm, due to the heuristic nature of this method. We obtained some outliers in the estimation of the parameters when the model structure is known. The mean and standard deviation of the damping factor $\hat{\zeta}$ and natural frequency $\hat{\omega}_n$ are 0.2853 ± 0.0564 and 9.2020 ± 2.7257 respectively.

Finally, we compute an estimation error, ε, to compare the methodologies presented in this paper:

$$\varepsilon = \frac{1}{n_{\mathrm{MC}}} \sum_{j=1}^{n_{\mathrm{MC}}} \left\| G_0(s) - \hat{G}_j(s) \right\|_2^2, \tag{33}$$

where n_{MC} is the number of MC simulations, $G_0(s)$ is the *true* CT transfer function and $\hat{G}_j(s)$ are the estimate TF for all MC simulations. This error for known model structure was 0.6801 and for Kautz BFs was 0.0205. We observe that using the Kautz BFs yield a smaller estimation error.

[2] In a practical case the complex pole can be estimated (Heuberger et al., 2005).

5. CONCLUSIONS

In this paper we addressed the problem of identification of CT systems with complex poles. We proposed an ML identification algorithm by using exact DT models and finite sample period. We extended the concept of *aliasing* in the likelihood function to deterministic systems. We also developed a recursive algorithm for constructing the DT versions of CT Kautz BFs. We observed that the log-likelihood function does not exhibit several local maxima when Kautz BFs are used to approximate CT systems. Our proposal exhibits good accuracy when Kautz BFs are used in the estimation algorithm for CT systems with complex poles utilising sampled-data.

REFERENCES

Audet, C. and Dennis, J.E. (2003). Analysis of generalized pattern searches. *SIAM Journal on Optimization*, 13(3), 889–903.

Baldelli, D., Mazzaro, M., and Peña, R.S. (2001). Robust identification of lightly damped flexible structures by means of orthonormal bases. *IEEE Transactions on Control Systems Technology*, 696–707.

Bernstein, D. (2009). *Matrix mathematics: theory, facts, and formulas: second edition.* Princeton University Press, 2 edition.

Bernstein, D. and So, W. (1993). Some explicit formulas for the matrix exponential. *IEEE Transactions Automatic Control*, 38(8), 1228–1232.

Chen, F., Agüero, J.C., Gilson, M., Garnier, H., and Liu, T. (2017). EM-based identification of continuous-time ARMA models from irregularly sampled data. *Automatica*, 77(3), 293 – 301.

Coronel, M., Carvajal, R., and Agüero, J.C. (2019). Identification of continuous-time deterministic system utilizing orthonormal basis functions and sample data. In *IEEE CHILEAN Conference on Electrical, Electronics Engineering, Information and Communication Technologies*.

Garnier, H. and Wang, L. (2008). *Identification of continuous-time models from sampled data.* Springer-Verlag London.

González, K., Coronel, M., Carvajal, R., Escárate, P., and Agüero, J.C. (2018). Maximum Likelihood identification of a continuous-time oscillator utilizing sampled data. *IFAC-PapersOnLine*, 51(15), 712–717. 18th IFAC Symposium on System Identification.

Goodwin, G., Agüero, J.C., Cea-Garrido, M.E., Salgado, M., and Yuz, J. (2013). Sampling and sampled-data models: the interface between the continuous world and digital algorithms. *IEEE Control Systems Magazine*, 33(5), 34–53.

Heuberger, P., van den Hof, P.M.J., and Bosgra, O. (1995). A generalized orthonormal basis for linear dynamical systems. *IEEE Transactions on Automatic Control*, 40(3), 451–465.

Heuberger, P., van den Hof, P.M.J., and Wahlberg, B. (2005). *Modelling and identification with rational orthogonal basis functions.* Springer-Verlag, London.

Jazwinski, A. (1970). *Stochastic processes and filtering theory.* Academic Press, San Diego, CA.

Kautz, W. (1954). Transient synthesis in the time domain. *IRE Trans. Circuit Theory*, 1, 29–39.

Kirshner, H., Maggio, S., and Unser, M. (2011). A sampling theory approach for continuous ARMA identification. *IEEE Transactions on Signal Processing*, 59(10), 4620–4634.

Laila, D. and Astolfi, A. (2006). Construction of discrete-time models for port-controlled Hamiltonian systems with applications. *Systems & Control Letters*, 55(8), 673–680. New Trends in Nonlinear Control.

Ljung, L. (1999). *System identification: theory for the User.* Prentice Hall PTR, Upper Saddle River, NJ, USA.

Ljung, L. and Wills, A. (2010). Issues in sampling and estimating continuous-time models with stochastic disturbances. *Automatica*, 46(5), 925 – 931.

Prior, A. and de Oliveira, P. (2014). Parameter estimation of a two regime stochastic differential model for a bilinear oscillator subjected to random loads. *Proc. of the 9th International Conference on Structural Dynamics*, 2845–2852.

Åström, K., Hagander, P., and Sternby, J. (1984). Zeros of sampled systems. *Automatica*, 20(1), 31 – 38.

Åström, K. and Wittenmark, B. (1984). *Computer-controlled systems: theory and design.* Prentice Hall, third edition.

Rojas, C., Yuz, J., Silva, C., and Rodriguez, J. (2014). Comments on "predictive torque control of induction machines based on state-space models". *IEEE Transactions on Industrial Electronics*, 61(3), 1635–1638.

Simos, T. (2008). The exact discrete model of a system of linear stochastic differential equations driven by fractional noise. *Journal of Time Series Analysis*, 29(6), 1019–1031.

Tzeng, C.Y., Wu, C.Y., and Chu, Y.L. (2001). A sensitivity function approach to the design of rudder roll stabilization controller. *Journal of Marine Science and Technology*, 9(2), 100–112.

Van Loan, C. (1978). Computing integrals involving the matrix exponential. *IEEE Transactions on Automatic Control*, 23(3), 395–404.

Wahlberg, B. (1988). Limit results for sampled systems. *International Journal of Control*, 48(3), 1267–1283.

Wahlberg, B. (1994). System identification using Kautz models. *IEEE Transactions on Automatic Control*, 39(6), 1276–1282.

Wahlberg, B. and Mäkilä, P. (1996). On approximation of stable linear dynamical systems using Laguerre and Kautz functions. *Automatica*, 32(5), 693–708.

Yuz, J., Alfaro, J., Agüero, J.C., and Goodwin, G.C. (2011). Identification of continuous-time state-space models from non-uniform fast-sampled data. *IET Control Theory Applications*, 5(7), 842–855.

Appendix A. LEMMAS

Lemma 4. Let A, $B \in \mathbb{R}^{m\times m}$ and $\bar{A}_{mr} \in \mathbb{R}^{mr\times mr}$. For $r \geq 2$, $\bar{A}_{mr}$ is defined by:

$$\bar{A}_{mr} = \mathrm{cut}(A, B, 0_{m\times m}, \cdots, 0_{m\times m}). \tag{A.1}$$

Then,

$$e^{\bar{A}_{mr}\Delta} = \mathrm{cut}(e^{A\Delta}, M_\Delta^1, M_\Delta^2, \cdots, M_\Delta^{r-1}), \tag{A.2}$$

where:

$$M_\Delta^1 = \int_0^\Delta e^{A(\Delta-\tau_1)} B e^{A\tau_1} d\tau_1, \tag{A.3}$$

$$M_{\Delta}^{k} = \int_0^{\Delta}\int_0^{\tau_1}\cdots\int_0^{\tau_{k-1}} e^{A(\Delta-\tau_1)}\left(\prod_{i=1}^{k-1} Be^{A(\tau_i-\tau_{i+1})}\right)$$
$$Be^{A\tau_k}d\tau_k d\tau_{k-1}\dots d\tau_1, \tag{A.4}$$

for $k \geq 2$ and $k = 2, \cdots, r-1$.

Proof. For $r = 2$.

$$\bar{A}_{2m} = \mathrm{cut}(A, B). \tag{A.5}$$

Utilising the result in (Bernstein, 2009, Sec. 11.14), the matrix exponential is given by:

$$e^{\bar{A}_{2m}\Delta} = \begin{bmatrix} e^{A\Delta} & \int_0^{\Delta} e^{A(\Delta-\tau_1)}Be^{A\tau_1}d\tau_1 \\ 0 & e^{A\Delta}\end{bmatrix}, \tag{A.6}$$

thus, it holds for $r = 2$.

Assume that the expression in (A.2) holds for $r = j$, where j is some positive integer greater than 2. Then, for $r = j+1$, we obtain:

$$\bar{A}_{m(j+1)} = \mathrm{cut}(A, B, 0, \cdots, 0) = \left[\begin{array}{c|c} A & \bar{B} \\ \hline 0_{mj\times mj} & \bar{A}_{mj}\end{array}\right]. \tag{A.7}$$

Utilising the result in (Bernstein, 2009, Sec. 11.14), the matrix exponential is given by:

$$e^{\bar{A}_{m(j+1)}\Delta} = \left[\begin{array}{c|c} e^{A\Delta} & \int_0^{\Delta} e^{A(\Delta-\tau_1)}\bar{B}e^{\bar{A}_{mj}\tau_1}d\tau_1 \\ \hline 0_{mj\times mj} & e^{\bar{A}_{mj}\Delta}\end{array}\right], \tag{A.8}$$

where:

$$\begin{aligned} A^* &= \int_0^{\Delta} e^{A(\Delta-\tau_1)}\bar{B}e^{\bar{A}_{mj}\tau_1}d\tau_1, \\ &= \int_0^{\Delta} e^{A(\Delta-\tau_1)}\left[Be^{A\tau_1}|BM_{\tau_1}^1|BM_{\tau_1}^2|\dots|BM_{\tau_1}^{j-1}\right]d\tau_1, \\ &= \Bigg[M_{\Delta}^1\Bigg|\int_0^{\Delta} e^{A(\Delta-\tau_1)}B\int_0^{\tau_1} e^{A(\tau_1-\tau_2)}Be^{A\tau_2}d\tau_2 d\tau_1\Bigg| \\ &\int_0^{\Delta} e^{A(\Delta-\tau_1)}B\int_0^{\tau_1}\int_0^{\tau_2} e^{A(\tau_1-\tau_2)}Be^{A(\tau_2-\tau_3)}Be^{A\tau_3}d\tau_3 \\ &d\tau_2 d\tau_1\Bigg|\cdots\Bigg|\int_0^{\Delta} e^{A(\Delta-\tau_1)}BM_{\tau_1}d\tau_1\Bigg], \\ &= \left[M_{\Delta}^1\middle|M_{\Delta}^2\middle|\cdots\middle|M_{\Delta}^j\right]. \end{aligned} \tag{A.9}$$

Finally, we obtain

$$e^{\bar{A}_{2j+2}\Delta} = \mathrm{cut}(e^{A\Delta}, M_{\Delta}^1, M_{\Delta}^2, \cdots, M_{\Delta}^j). \tag{A.10}$$

Thus, by mathematical induction, (A.2) holds for all positive integer r greater than 2. □

Remark 5. Notice that Lemma 4 is an extension of the result presented in Van Loan (1978) for r blocks of matrices. ▽

Lemma 6. Let $A, B \in \mathbb{R}^{m\times m}$ and $P \in \mathbb{R}^{mr\times mr}$

$$P = \mathrm{cut}(A, B), \tag{A.11}$$

if A is nonsingular matrix, then the inverse of P is given by:

$$P^{-1} = \mathrm{cut}(A^{-1}, -A^{-1}BA^{-1}). \tag{A.12}$$

Proof. See (Bernstein, 2009, Proposition 2.8.4). □

Appendix B. THEOREM

The input-output representation of the state-space form in (25) is given by:

$$F^d(z) = C\left(zI - A^d\right)^{-1}B^d. \tag{B.1}$$

(1) **For** $i = 1$ Directly using the definition (B.1) and the matrix exponential (see Bernstein and So (1993)). □

(2) **For** $i \geq 2$. First if $m = 2$ and $i = 2$.

$$\bar{A}_4 = \mathrm{cut}(A_{\bar{W}}, B^*),\ \ \bar{B}_4 = [0_{2\times 2}\ \ N]^T,\ \ \bar{C}_4 = [L\ \ 0_{2\times 2}], \tag{B.2}$$

where: $A_{\bar{W}}$ and B^* are given in (24), $L = [1\ 0]$ and $N = [0\ 1]^T$.

Based on Lemmas 4 and 6 and replacing (B.2) in (B.1), we obtain:

$$\begin{aligned} \bar{F}_4^d &= [L\ 0_{2\times 2}]\begin{bmatrix} R & -M_{\Delta}^1 \\ 0 & R\end{bmatrix}^{-1}\int_0^{\Delta}\begin{bmatrix} e^{A_{\bar{W}}\eta} & M_{\eta}^1 \\ 0 & e^{A_{\bar{W}}\eta}\end{bmatrix}\begin{bmatrix}0_{2\times 2} \\ N\end{bmatrix}d\eta, \\ &= [1\ 0]\left(R^{-1}B_{d_1} + R^{-1}M_{\Delta}^1R^{-1}B_{d_0}\right), \end{aligned} \tag{B.3}$$

where: $R = z - e^{A_{\bar{W}}\Delta}$ and:

$$B_{d_1} = \int_0^{\Delta} M_{\eta}^1 N d\eta,\ \ B_{d_0} = \int_0^{\Delta} e^{A_{\bar{W}}\eta}Nd\eta. \tag{B.4}$$

Finally,

$$F_4^d(z) = F_2^d(z) + \bar{F}_4^d(z), \tag{B.5}$$

thus, it holds for $i = 2$.

Assume that expression in (29) holds for $i = j$, where j is some positive integer greater than 2. Then, for $m = 2$ and $i = j+1$, we obtain:

$$\bar{A}_{2j+2} = \mathrm{cut}(A_{\bar{W}}, B^*, 0_{2\times 2}, \cdots, 0_{2\times 2}), \tag{B.6}$$

$$\bar{B}_{2i} = [0_{2\times 2}\ 0_{2\times 2}\ \dots\ N]^T, \bar{C}_{2i} = [L\ 0_{2\times 2}\ \cdots\ 0_{2\times 2}]. \tag{B.7}$$

Based on Lemmas 4 and 6 and replacing (B.7) in (B.1), we obtain:

$$\begin{aligned} \bar{F}_{2j+2}^d(z) &= \bar{C}_{2i}\Big[\mathrm{cut}(R, -M_{\Delta}^1, -M_{\Delta}^2, \cdots, -M_{\Delta}^j)\Big]^{-1} \\ &\int_0^{\Delta}\mathrm{cut}(e^{A_{\bar{W}}\eta}, M_{\Delta}^1, M_{\Delta}^2, \cdots, M_{\Delta}^j)\,[0_{2\times 2}\ 0_{2\times 2}\ \cdots\ N]^T d\eta, \\ &= \bar{C}_{2i}\begin{bmatrix} R^{-1} & R^{-1}M^*R^{-1} \\ 0_{2j\times 2j} & \mathcal{A}_{2j}^{-1}\end{bmatrix}\left[B_{d_j}\ B_{d_{j-1}}\ \cdots\ B_{d_0}\ B_{d_0}\right]^T, \end{aligned} \tag{B.8}$$

where:

$$\mathcal{A}_{2j}^{-1} = \mathrm{cut}(R^{-1}, R^{-1}M_{\Delta}^1R^{-1}, \cdots, R^{-1}M_{\Delta}^{j-1}R^{-1}). \tag{B.9}$$

Then

$$\bar{F}_{2j+2}^d(z) = [1\ 0]\left(R^{-1}B_{d_j} + \sum_{k=1}^{j} R^{-1}M_{\Delta}^kR^{-1}B_{d_{j-k}}\right). \tag{B.10}$$

$$B_{d_0} = \int_0^{\Delta} e^{A_{\bar{W}}\eta}Nd\eta,\ B_{d_l} = \int_0^{\Delta} M_{\eta}^l N d\eta,\ l = 1, \cdots, r-1.$$

For $F_{2i-1}^d(z)$ the proof is similar with the change $N = [1\ 0]^T$.

We show, by mathematical induction, that (28) and (29) are correct for all positive integer i greater than 2. □